FULL PAPER

Magnetic Resonance in Medicine 00:00–00 (2013)

Adiabatic Inversion Pulses for Myocardial T1 Mapping

Peter Kellman,[1]* Daniel A. Herzka,[2] and Michael Schacht Hansen[1]

Purpose: To evaluate the error in T1 estimates using inversion-recovery-based T1 mapping due to imperfect inversion and to perform a systematic study of adiabatic inversion pulse designs in order to maximize inversion efficiency for values of transverse relaxation (T2) in the myocardium subject to a peak power constraint.

Methods: The inversion factor for hyperbolic secant and tangent/hyperbolic tangent adiabatic full passage waveforms was calculated using Bloch equations. A brute-force search was conducted for design parameters: pulse duration, frequency range, shape parameters, and peak amplitude. A design was selected that maximized the inversion factor over a specified range of amplitude and off-resonance and validated using phantom measurements. Empirical correction for imperfect inversion was performed.

Results: The tangent/hyperbolic tangent adiabatic pulse was found to outperform hyperbolic secant designs and achieve an inversion factor of 0.96 within $\pm$150 Hz over 25% amplitude range with 14.7 μT peak amplitude. T1 mapping errors of the selected design due to imperfect inversion was $\sim$4% and could be corrected to $<$1%.

Conclusions: Nonideal inversion leads to significant errors in inversion-recovery-based T1 mapping. The inversion efficiency of adiabatic pulses is sensitive to transverse relaxation. The tangent/hyperbolic tangent design achieved the best performance subject to the peak amplitude constraint. **Magn Reson Med 000:000–000, 2013. © 2013 Wiley Periodicals, Inc.**

Key words: MRI; adiabatic inversion; T1 mapping; MOLLI

INTRODUCTION

T1 mapping in the myocardium provides a means for quantifying and detecting edema and/or fibrosis with elevated T1 (1–5). "Look-Locker" methods such as modified Look-Locker inversion-recovery (MOLLI) approach (6,7) based on inversion recovery assume a complete idealized inversion. It is generally appreciated that there is considerable spatial variation in transmit field strength ($B1^+$). Even at 1.5 T commonly used for cardiac MRI, the variation can be as high as 25%. To mitigate this problem, adiabatic inversion pulses (8–14) are often used to reduce the sensitivity to $B1^+$ inhomogeneity in cardiac applications such as Gadolinium-enhanced imaging (15,16) and parametric mapping. The hyperbolic secant (HS) design (12) has been used extensively and provides excellent inversion homogeneity over a wide range of both $B1^+$ and off-resonance (B0). However, although the inversion is homogeneous, it is not necessarily complete, which has important implications for the accuracy of T1 mapping.

Quantitative measurement of T1 based on inversion recovery leads to more stringent demands on the performance of the inversion. In this study, the effect of imperfect inversion on T1 measurement accuracy is characterized, and we perform a systematic study of the choice of design parameters used in adiabatic inversion pulses. Adiabatic inversion pulses used to mitigate inhomogeneity of transmit B1 field strength do not achieve perfect inversion as a result of transverse relaxation (T2) during the pulse (14). Shorter duration inversion pulses achieve better inversion but require higher peak power which may not be realizable. The trade-off of peak power versus inversion efficiency for various designs (12) has shown that designs which deliver more constant power achieve a specified inversion at a reduced peak power. However, these studies have not explicitly accounted for transverse relaxation. By incorporating realistic physiological tissue parameters (T1 and T2) into the design, it is possible to choose parameters with improved inversion efficiency for the specified design criteria (i.e., peak voltage, off-resonance bandwidth, and transmit B1 variation).

Imperfect adiabatic inversion is T2 dependent and leads to a T2-dependent error in inversion-recovery-based T1 estimates. A reduced T2 dependence is achieved as well as improved inversion efficiency by careful choice of design parameters. Empirical correction for imperfect adiabatic inversion may be used to further improve T1 measurement accuracy.

In addition to imperfect inversion, the MOLLI method incurs a number of errors in estimating T1. The use of a Look-Locker correction, which is an approximation (6,7), leads to estimates of T1 that are sensitive to the tissue T1 and T2, off-resonance, heart rate, as well as imaging protocol parameters such as the sampling strategy, flip angle, and matrix size. This study relates solely to the contribution of error to the inversion preparation.

THEORY

Influence of Imperfect Inversion

Inversion recovery is widely used for T1 mapping using Look-Locker methods. In applications such as cardiac MR, a modified Look-Locker (MOLLI) method (6,7) uses inversion recovery with multiple single-shot images at

[1]National Institutes of Health, Department of Health and Human Services, National Heart, Lung and Blood Institute, Bethesda, Maryland, USA.

[2]Department of Biomedical Engineering, Johns Hopkins School of Medicine, Baltimore, Maryland, USA.

Grant sponsor: NIH/NHLBI Intramural Research Program.

*Correspondence to: Peter Kellman, Ph.D., National Heart, Lung and Blood Institute, National Institutes of Health, Room B1D416, Building 10, 10 Center Drive, MSC-1061, Bethesda, MD 20892-1061. E-mail: kellman@nih.gov

Received 8 January 2013; revised 18 March 2013; accepted 11 April 2013

DOI 10.1002/mrm.24793

Published online in Wiley Online Library (wileyonlinelibrary.com).

different inversion times (TIs). Pixelwise parametric mapping is accomplished by performing a curve fit to the multiple TI measurements. The original MOLLI study (6) assumes a three-parameter model of the form $S(\mathrm{ti}) = A - B\exp(-\mathrm{ti}/\mathrm{T1}^*)$, where $\mathrm{T1}^* < \mathrm{T1}$ represents the apparent T1 which is shortened by the influence of imaging radiofrequency pulses. The desired T1 is then calculated at each pixel using $\mathrm{T1} = \mathrm{T1}^*(B/A - 1)$, referred to as the Look-Locker correction, originally derived from considering a continuous fast low-angle shot gradient echo readout (17,18). The Look-Locker correction is used in MOLLI method despite the fact that imaging uses non-continuous balanced steady state free precession (SSFP), which violates the assumption used in the formulation because fast low-angle shot (FLASH) is noncoherent steady-state imaging and therefore insensitive to T2, whereas balanced steady-state free precession is coherent steady-state imaging and carries significant T2 weighting. This assumption is a key source of error not treated in this study and is sensitive to variables such as T1 and T2 as described in the literature (6,19,20). In the prior formulations, a perfect inversion is assumed. The effect of imperfect inversion introduces a further error, which is the subject of this work.

In the original formulation for continuous FLASH imaging proposed by Deichmann and Haase (17), the equation for the recovery of magnetization over time after an ideal inversion is as follows:

$$M(t) = \mathrm{M0}^* - (\mathrm{M0} + \mathrm{M0}^*)\exp(-t/\mathrm{T1}^*), \quad [1]$$

with $\mathrm{M0}^* = \mathrm{M0}$ (T1*/T1) representing the steady-state magnetization, and T1* representing the apparent T1 controlling relaxation from the inverted equilibrium magnetization to M0*. This is fit to a three-parameter model $M(t) = A - B\exp(-t/\mathrm{T1}^*)$, where the coefficients become $A = \mathrm{M0}^* = \mathrm{M0}$ (T1*/T1) and $B = (\mathrm{M0} + \mathrm{M0}^*) = \mathrm{M0}$ (1 + T1*/T1). The Look-Locker correction is readily solved as $\mathrm{T1}/\mathrm{T1}^* = B/A - 1$. With imperfect inversion, Eq. [1] may be rewritten as follows:

$$M(t) = \mathrm{M0}^* - (\delta\mathrm{M0} + \mathrm{M0}^*)\exp(-t/\mathrm{T1}^*), \quad [2]$$

with the inversion factor $\delta = |Mz/\mathrm{M0}| \leq 1$ with Mz measured at the end of the inversion pulse. In this case, $B = (\delta\ \mathrm{M0} + \mathrm{M0}^*) = \mathrm{M0}$ (δ + T1*/T1), and the Look-Locker correction becomes $\mathrm{T1}/\mathrm{T1}^* = (B/A - 1)/\delta$. In other words, if the adiabatic inversion is imperfect, then the Look-Locker correction must include an additional $1/\delta$ factor or else a significant error in estimated T1 may result. This correction factor is of particular importance when performing T1 mapping in short T2 species, as transverse relaxation causes imperfect inversion.

Correction for imperfect inversion by incorporating an empirical factor relating to the adiabatic inversion pulse is possible. T1 estimates for MOLLI method are not typically corrected for the inversion and may be denoted as $\mathrm{T1}_{\mathrm{uncorrected}} = (B/A - 1)\mathrm{T1}^*$. The proposed corrected estimate $\mathrm{T1}_{\mathrm{corrected}} = (B/A - 1)\mathrm{T1}^*/\delta$ is simply scaled by a fixed value of the inversion factor δ, which is calculated at a nominal value of T1 and T2. However, the inversion factor $\delta = \delta(\mathrm{T1}, \mathrm{T2})$ is dependent on both T1 and T2; it is therefore desirable to use an adiabatic design that has better inversion efficiency which will also minimize the sensitivity of the correction to the unknown tissue parameters.

Adiabatic Inversion

Adiabatic pulses may be used to achieve inversion that is fairly independent of the pulse amplitude above a certain threshold. The adiabatic designs considered in this study were the HS (8) and the tangent/hyperbolic tangent (tan/tanh). The HS may be generalized as the HSn by which flattens the amplitude thereby delivering more constant power. The formulation of the amplitude and phase for the HSn (10,12) is as follows:

$$B(t) = B1_{\max}(\beta\tau^n), \quad [3]$$

$$\varphi(t) = K\int\int B1^2(\tau)\mathrm{d}\tau, \quad [4]$$

where K is a constant that determines the frequency sweep bandwidth, and $-1 \leq t \leq 1$, $\tau = 2t/T$. The constant β determines the amplitude level at the start and end of the pulse and is typically chosen such that $\mathrm{sech}(\beta) = 0.1$ (10,12). The phase is calculated by numerical integration of the amplitude envelope and scaled to obtain the desired swept frequency range ($\pm f_{\max}$). The HS pulse is denoted as HS1 with $n = 1$. Design parameters for the HSn are the exponent n, duration T, peak amplitude $B1_{\max}$, frequency sweep $f_{\max}$, and constant β.

The tan/tanh design of the adiabatic full passage pulse is synthesized by concatenating the half-passage and reverse half-passage waveforms. The amplitude and phase for the reverse half-passage may be calculated as follows (9):

$$\mathrm{B1}(t) = \mathrm{B1}_{\max}\tanh[\zeta(1 - t)/T] \quad [5]$$

$$\phi(t) = \phi_{\max} - [(2 \times \pi \times f_{\max} \times T)/\kappa\tan(\kappa)]\ln[\cos(\kappa t/T)/\cos(\kappa)] \quad [6]$$

with $0 < t \leq T$. Design parameters for the tan/tanh are the duration T, peak amplitude $\mathrm{B1}_{\max}$, frequency sweep $f_{\max}$, and constants ζ and κ.

METHODS

Adiabatic Inversion Design Optimization

The inversion factor was calculated for each adiabatic inversion design using Bloch equations. Optimization was performed by brute force over a range of design parameters. The design space was ±150 Hz and 25% variation in B1 field strength with a peak voltage constraint. The 25% amplitude range at 1.5 T in the heart was based on a limited study ($n = 4$), which measured the variation in flip angle at 1.5 T using a saturated dual-flip-angle method (21). In this study (unpublished), data were acquired using two flip angles acquired on separate breath-holds using an adiabatic BIR-4 saturation pulse for each heart beat and a gradient recalled echo (GRE) echoplanar imaging (EPI) (echo train length 8) readout with single excitation per heartbeat. The actual flip angle was always found to be less than the prescribed flip

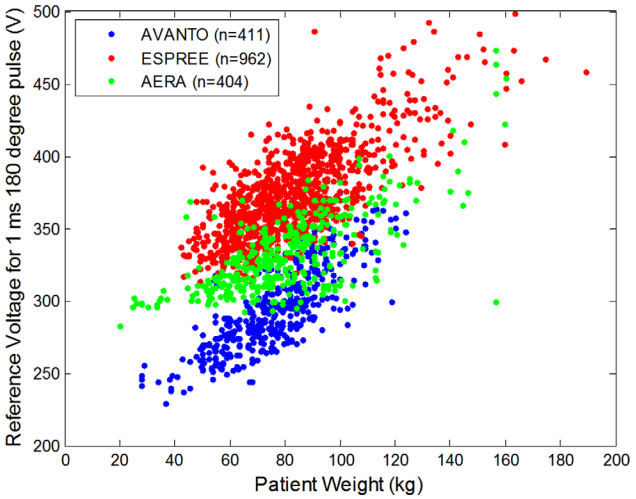

FIG. 1. Transmit amplifier reference voltage as measured by scanner flip angle calibration required to achieve a 180° flip angle using a 1-ms square pulse for a range of subject loading for three MR systems. These voltages correspond to a 11.7 μT $B1^+$ field. [Color figure can be viewed in the online issue, which is available at wileyonlinelibrary.com.]

angle, i.e., 25% variation defined as being in the range 0.8–1.0 times the prescribed flip angle. At 3 T, the variation in transmit flip angle is significantly greater, varying as much as 32–63% ($n = 10$) across the left ventricle (LV) (22). The off-resonance variation across the heart may be significant due in large part to the interface between the heart and lung. The maximum deviation of off-resonance frequency variation across the LV at 1.5 T was determined to be 83 ± 36 Hz ($n = 20$) in a study (unpublished data) of quality assurance data with analysis approved by the NIH Office of Human Subject Research. Field map measurements were made as a byproduct of water fat separated imaging reconstruction using a multiecho GRE sequence with nonlinear least squares reconstruction (23). The off-resonance variation may be reduced by localized shimming. As the balanced steady-state free precession imaging sequence used in T1 mapping using the MOLLI approach is sensitive to off-resonance frequency (e.g., usable range $< \pm 1/2TR$ with TR on order of 3 ms), a ±150 Hz requirement for uniform inversion was deemed adequate to not further limit the accuracy due to off-resonance in the heart.

The peak voltage of radiofrequency pulses is limited by both amplifier and specific absorbtion rate (SAR). In our experience, the amplifier constraint is the dominant limitation for this sequence as the inversion pulse occurs only every few heartbeats. The transmit voltage to achieve a specified B1 field is both system and patient dependent. Figure 1 shows the transmitter reference voltage required to achieve a 180° flip angle with a 1 ms pulse, corresponding to a B1 of 11.7 μT. The data were recorded for the purpose of quality control and is plotted for a large number of subjects imaged on three different 1.5 T scanners with different bore lengths and diameters. These quality assurance data (analysis approved by the NIH Office of Human Subject Research) serve as reference in selecting a design that will achieve the desired inversion efficiency over a wide range of subject loading. The highest reference voltages were required using the wide, short-bore scanner (Siemens Espree, Siemens Medical Solutions, Erlangen, Germany); for this model, the maximum amplifier voltage was determined to be ~650 V, which is 1.3 times 500 V, which was the maximum reference voltage for the heaviest patients with greatest loading. Therefore, a worst-case limitation on peak B1 is 1.3×11.7 μT or ~15 μT.

In view of the demands to achieve ideal inversion for quantitating T1 at low T2s representative of the myocardium, we revisit the performance of various adiabatic inversion pulses. The design considered HSn and tan/tanh pulses over the range T1 = 400–1600 ms and T2 = 45–250 ms. Design optimization included the pulse duration, frequency sweep bandwidth, and shape parameters. For each pulse design considered, the inversion factor was calculated for 30 frequencies across ±150 Hz and 20 B1 field amplitudes between 80 and 100% of the maximum constraint. The design considered five maximum voltages corresponding to 1, 1.25, 1.5, 1.75, and 2 times the reference voltage for a 1-ms 180 pulse equivalent to B1 field strengths of 11.7, 14.7, 17.6, 20.5, and 23.5 μT. For HSn designs, the parameters were as follows: $n = 1$, 2, 4, and 8; duration = 2.56, 5.12, and 10.24 ms; one-sided frequency sweep $f_{max} = 250$–5000 Hz in 200 Hz steps; and $\beta = \text{asech}(x)$ in 16 steps, $x = 0.005$–0.08. For tan/tanh designs, the parameters were as follows: duration = 1.28, 2.56, and 5.12 ms; one-sided frequency sweep $f_{max} = 7000$–15,000 Hz in 1000 Hz steps; $\zeta = 8$–20 in steps of 2; and $\tan(\kappa)$ from 10 to 30 in steps of 2. The brute-force search selected the set of design parameters that had the highest inversion factor calculated over the full range of frequency and amplitude calculated at 600 amplitude and frequency pairs times 5 peak voltages for each set of parameters. There were $4 \times 3 \times 24 \times 16 = 4608$ HSn designs and $3 \times 9 \times 7 \times 11 = 2079$ tan/tanh designs. Design optimization was performed at the minimum T2 = 45 ms with fixed T1 = 1000 ms.

Phantom Validation

Experimental validation used a set of $CuSO_4$-doped agar gel phantoms with varying concentrations with T1 and T2 in the expected range for myocardium, both native and with Gd contrast. Measurements were acquired using a custom research inversion-recovery spin-echo (SE) sequence with TR = 10 s at multiple TIs using a 1.5 T MAGNETOM Aera Scanner (Siemens Medical Solutions), which enabled testing of several inversion pulse designs. The T1 and the inversion factor δ were estimated using a three-parameter fit, i.e., $M(t) = M0[1 - (1 + \delta)\exp(-t/T1)]$, which assumes complete relaxation (TR << T1) and the inversion factor is denoted by δ. T2 was measured using exponential fit to SE measurements with TR = 10 s and varying echo times. Transmit field strength was measured using the dual-flip-angle method (24) to ensure the correct transmit power level, and off-resonance was measured using a multiecho GRE

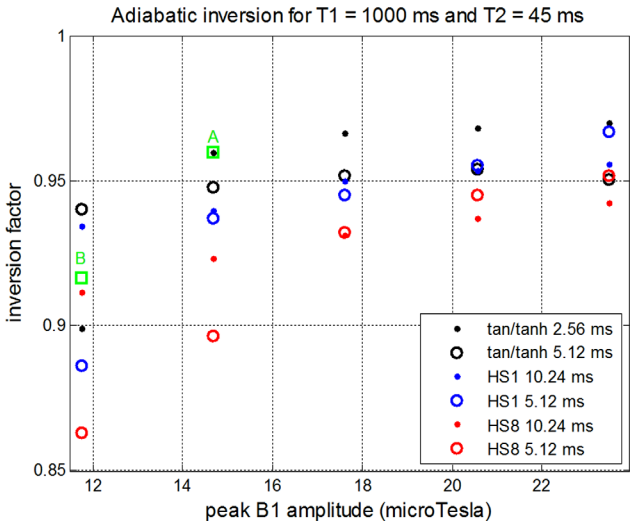

FIG. 2. Inversion factor versus peak B1 amplitude calculated for various adiabatic inversion pulse designs. Designs marked by green box A and B correspond to the T1 mapping optimized tan/tanh and the HS1 used on the system product sequences, respectively. [Color figure can be viewed in the online issue, which is available at wileyonlinelibrary.com.]

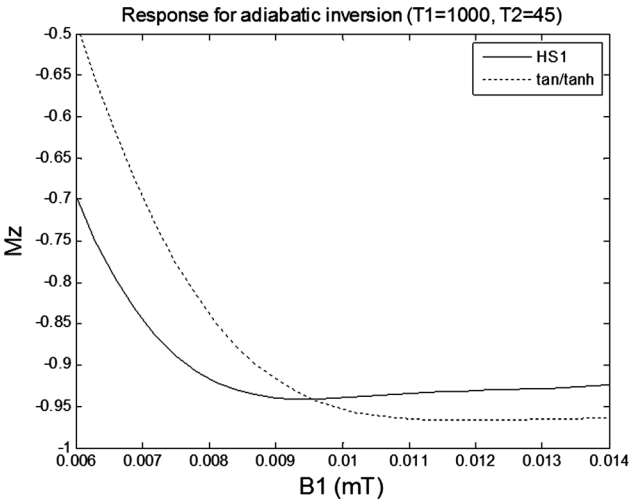

FIG. 3. Responses of inversion pulse illustrating imperfect inversion due to T2 relaxation. [Color figure can be viewed in the online issue, which is available at wileyonlinelibrary.com.]

field mapping sequence to ensure that the data were acquired on-resonance.

T1 Correction for Imperfect Inversion

The proposed empirical correction was applied to the SE T1 estimate as described below to emulate the Look-Locker correction used in the MOLLI method without incurring other errors that affect MOLLI method, namely the use of balanced steady-state free precession imaging as well as the influence of successive measurements on previous measurements. In this manner, the error due to imperfect inversion may be separated from the other errors that confound MOLLI method. Define the T1 estimate ($T1_{SE}$) using the SE sequence as the apparent T1 from the three-parameter fit $S(t) = A - B\ \exp(-t/T1_{SE})$ as there is negligible influence between measurement using a long TR >> T1. In the case of SE imaging, a Look-Locker correction $(B/A - 1)$ as used in the MOLLI method is unnecessary; for perfect inversion, the factor $B/A - 1 = 1$, and for imperfect inversion, $B/A - 1 = \delta$. However, to calculate the effect of imperfect inversion due to the Look-Locker correction used in MOLLI method, the correction $(B/A - 1)$ was applied to the apparent $T1_{SE}$ with and without the added empirical correction factor δ. The Look-Locker-corrected SE estimates, which serve as surrogates for the analysis of MOLLI method error due to the inversion pulse, may be further corrected for the imperfect adiabatic inversion. These estimates were defined as: $T1_{uncorrected} = (B/A - 1)\ T1_{SE}$ and $T1_{corrected} = (B/A - 1)T1_{SE}/\delta$, where $\delta = \delta(T1, T2)$ was the inversion factor calculated for T1 = 1000 and T2 = 45 ms, taken as approximate values for native myocardium. Absolute and percent errors were computed against the relaxation time $T1_{SE}$ as the ground truth.

RESULTS

The inversion factor calculated for a variety of designs (Fig. 2) shows that for short T2 = 45 ms, the inversion factor is significantly improved (closer to ideal) for the tan/tanh design with duration 2.56 ms (black dots) than any of the HS*n* designs for all specified peak B1 amplitudes that are greater than 14 μT. The best HS1 design would require almost twice the peak amplitude to achieve the same inversion factor. The HS1 outperformed the HS8 at this low value of T2. A tan/tanh design marked by the green box labeled with "A" [$f_{max} = 9.5$ kHz, $\zeta = 10$, $\tan(\kappa) = 22$] was selected as it achieved an inversion factor of 0.96 for 14.7 μT, which was realizable on all scanners under worst-case patient loading conditions (with peak amplitude ~25% higher than the reference voltage in Fig. 1). The HS1 design marked by the green box labeled with "B" (10.24 ms, $f_{max} = 535$ Hz, $\beta = 3.42$) was chosen for experimental comparison as this design was used in a previously reported MOLLI implementation (7). Adiabatic inversion pulses are used in HS1 designs to produce homogenous inversion over a wide bandwidth and are widely used across many platforms. This specific HS1 with an inversion factor of 0.92 at 11.7 μT is used more generally on our system and was designed to a different criterion at a reduced peak amplitude. This HS1 design does not achieve the best inversion factor for the specified design criteria used here, but rather has higher bandwidth.

The adiabatic condition achieves independence of B1 transmit field strength but does not achieve perfect inversion (Fig. 3) due to T2 relaxation during the pulse, shown for both HS1 design "B" and tan/tanh design "A" on-resonance. The magnetization (Mz) versus B1 and off-resonance is graphed (Fig. 4) for both designs. Note the contours that indicate the inversion factor; the optimized pulse achieves improved inversion over the design region indicated by the dotted green box. The inversion factor $\delta(T1, T2)$ is dependent on both T1 and T2 (Fig. 5). The tan/tanh design exhibits both higher inversion factor

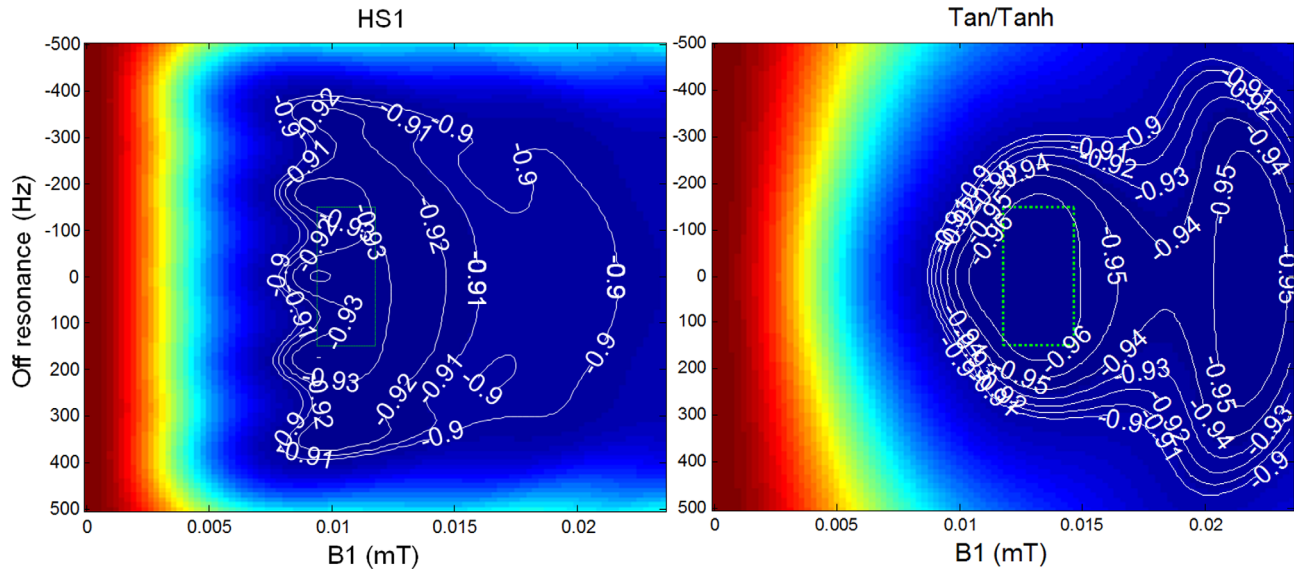

FIG. 4. Response of adiabatic inversion pulse for T1 = 1000 ms and T2 = 45 ms using HS1 design "B" (left) and tan/tanh (right) design "A." Design region is indicated by dotted green box (25% amplitude range, ±150 Hz).

as well as greatly reduced sensitivity to T1 and T2 when compared with the HS1 design. For the tan/tanh design "A," the inversion factor varies from 0.96 to 0.99 over a wide range of T2 from 40 to 250 ms, with very little variation with T1 from 400 to 1600 ms, whereas the HS1 design "B" varies considerably with both T1 and T2 (Fig. 5).

Phantoms were constructed with T1 and T2 in the range expected for myocardium, and T1 and T2 were measured using a SE sequence (Fig. 6). The measured inversion factor based on the three-parameter fit is greatly improved for the tan/tanh design (Fig. 7) when compared with the HS1 reducing the uncorrected error in myocardial T1 from ~10% to <5%. Figure 7 shows both the measured and simulated inversion factors for each phantom, in which the simulated data are calculated for each phantom using the corresponding measured T1 and T2 (Fig. 6c).

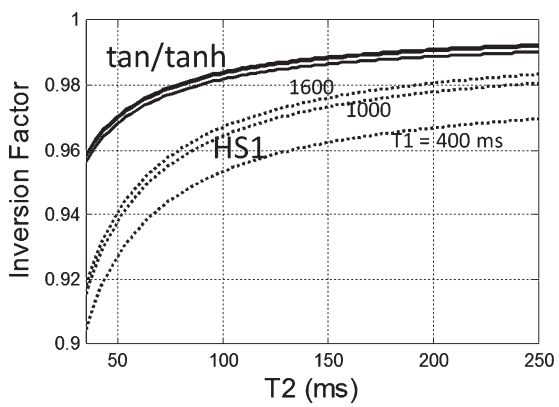

FIG. 5. Dependence of adiabatic inversion factor on T2 for 10.24 ms HS1 design "B" (dashed) and 2.56 ms tan/tanh design "A" (solid) designs for T1 = 400, 1000, and 1600 ms. Note that design "A" has both higher inversion factor as well as reduced sensitivity to T1 and T2.

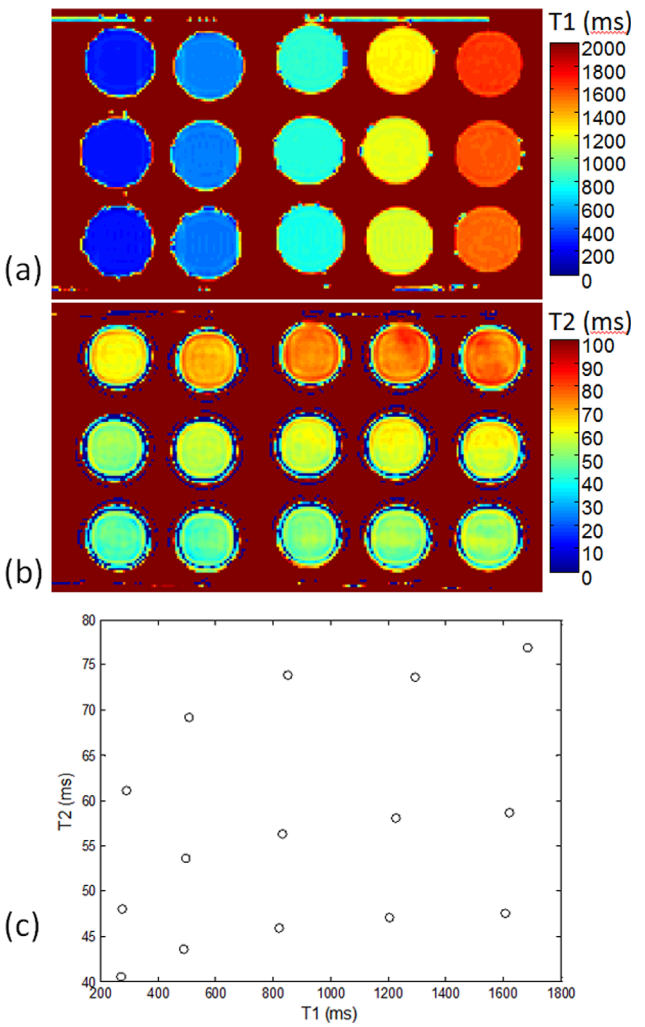

FIG. 6. Measurements of phantom T1 and T2: (**a**) T1 map, (**b**) T2 map, and (**c**) T1 and T2 values for each phantom tube.

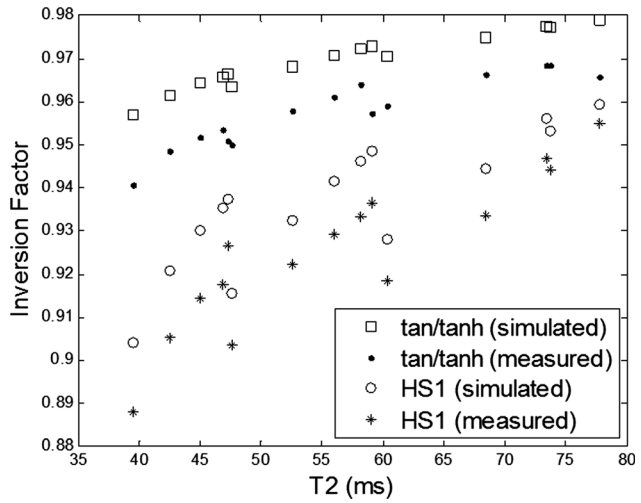

FIG. 7. Measured and simulated inversion factor versus T2 (various T1) for phantom data using tan/tanh design "A" and HS1 design "B." Simulated values are calculated based on measured phantom T1 and T2 (Fig. 6c).

Empirical correction may be applied to T1 maps to reduce the error due to imperfect inversion. The estimated T1 after Look-Locker correction versus true T1 measured by SE with and without empirical correction for imperfect inversion for both HS1 and tan/tanh designs (Fig. 8) shows that the T2-dependent correction leads to a reduced error for the tan/tanh design. For the tan/tanh pulse design "A," imperfect inversion leads to a T1 error of ~4%, which may be corrected within 1% over the range of T1 and T2 values tested. The HS1 design "B" has an error of ~10% and may be corrected to within ~3%, leading to overcorrection using this method.

DISCUSSION AND CONCLUSIONS

Adiabatic inversion pulses are commonly used to achieve homogeneous inversion over a range of transmit field strengths. Imperfect adiabatic inversion results from transverse relaxation (T2) during the pulse and may result in an error in estimates of T1 using inversion-recovery methods such as MOLLI (6,7) or other schemes that assume perfect inversion independent of the method of image readout. T1 mapping error due to imperfect inversion leads to an underestimation of T1 and compounds other sources of error which also tend to underestimate. Underestimation in the MOLLI approach (19,20) generally results from the approximation of the Look-Locker correction using SSFP readout with noncontinuous readout and is sensitive to tissue T1 and T2, off-resonance, heart rate, and a number of protocol parameters such as sampling strategy, flip angle, and matrix size. These errors lead to systematic bias errors that range from 5 to 10%, not including the error due to imperfect inversion. The proposed adiabatic pulse design and proposed correction reduces the error by ~8% when compared with the currently widely used HS design without correction. It improves the reproducibility by reducing the sensitivity of the inversion factor to T1 and T2. There is currently an active discussion over the magnitude of the error and what accuracy is required in order to be clinically useful. Clinical applications (1–4) are emerging that are based on subtle changes in apparent T1 to detect diffuse disease processes both in individuals and population studies. This study is aimed at improving the overall accuracy and developing a better understanding of an important factor that contributes to the overall error.

The measured values for inversion factor are systematically biased relative to the simulated values (Fig. 7). The measured factors are between 0.014 (T2 = 40 ms) and 0.009 (T2 = 80 ms) less than the simulated values for the proposed tan/tanh design "A," and similarly 0.016 (T2 = 40 ms) and 0.006 (T2 = 80) less for the HS1 design "B." The resulting approximate 1% discrepancy between the measurement and simulation may be due to experimental error or possibly due to the simulation model not accounting for all effects that influence inversion efficiency. Although this discrepancy is not fully resolved, the inversion factor of the proposed design is clearly improved by a significant amount when compared with the current HS1 design.

A systematic study of the design of adiabatic inversion pulses was undertaken with the goal of reducing the

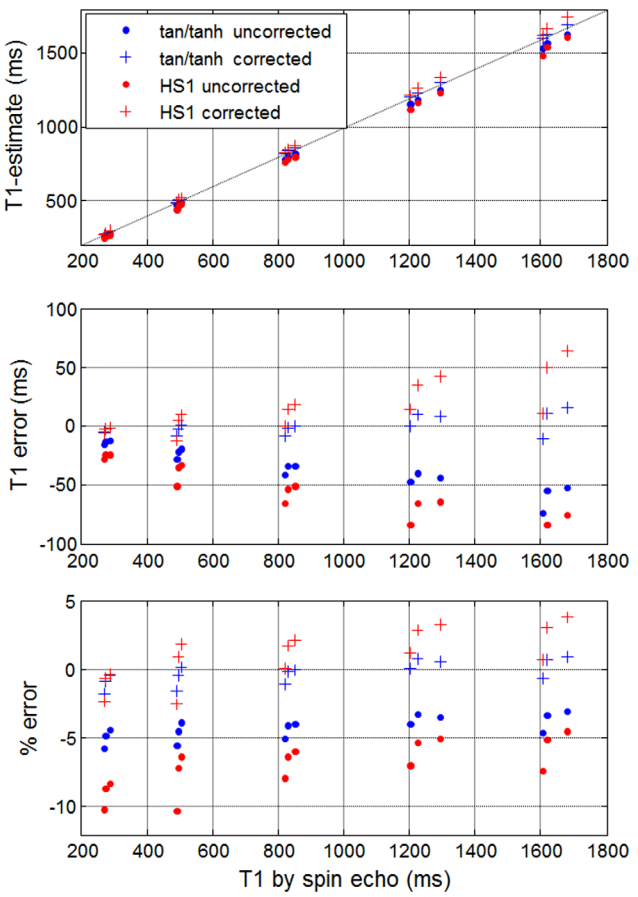

FIG. 8. Estimated T1 after "Look-Locker" correction versus true T1 measured by spin echo with and without empirical correction for imperfect inversion for both the HS1 design "B" and tan/tanh design "A." [Color figure can be viewed in the online issue, which is available at wileyonlinelibrary.com.]

quantitative error in T1 mapping. The inversion efficiency may be improved by using a shorter duration pulse with optimized parameters. Because of the peak power constraints, a tan/tanh design was found to achieve better inversion performance than HS*n* designs. Note that we use the term inversion factor δ (also referred to as inversion number l_0; Ref. 13)), which is related to inversion efficiency defined as $e = 1/2(1 + \delta)$ in much of the literature on adiabatic pulses (13,14). Although it is reported (10–14) that the HS8 has a significant reduction in peak B1 strength relative to the HS1 to achieve a specified inversion factor, this relationship does not account for T2 relaxation during the pulse. For T2 on the order of 45 ms, relaxation has a strong effect on the inversion performance and leads to a different design choice. This study was limited to design optimization of HS*n* and tan/tanh pulses with analytic expressions. Numerically optimized pulses (13,25) might offer further performance improvement.

Reduced dependence on both T1 and T2 facilitate a calibrated empirical correction of T1 estimates to further reduce the T1 error observed during T1 mapping due to imperfect inversion. Although it is possible to estimate the inversion parameter directly in the T1 mapping sequence by acquiring additional images without inversion and performing a four-parameter fit, this approach requires considerably longer acquisition and further sacrifices precision due to the noise sensitivity with added degrees of freedom (26).

REFERENCES

1. Flett AS, Hayward MP, Ashworth MT, Hansen MS, Taylor AM, Elliott PM, McGregor C, Moon JC. Equilibrium contrast cardiovascular magnetic resonance for the measurement of diffuse myocardial fibrosis: preliminary validation in humans. Circulation 2010;122:138–144.
2. Broberg CS, Chugh S, Conklin C, Sahn DJ, Jerosch-Herold M. Quantification of diffuse myocardial fibrosis and its association with myocardial dysfunction in congenital heart disease. Circ Cardiovasc Imaging 2010;3:727–734.
3. Schelbert E, Testa SM, Meier CG, et al. Myocardial extracellular volume fraction measurement by gadolinium cardiovascular magnetic resonance in humans: slow infusion versus bolus. J Cardiovasc Magn Reson 2011;13:16.
4. Ugander M, Oki AJ, Hsu L-Y, Kellman P, Greiser A, Aletras AH, Sibley CT, Chen MY, Bandettini WP, Arai AE. Extracellular volume imaging by MRI provides insight into overt and subclinical myocardial pathology. Eur Heart J 2102;33:1268–1278.
5. Kellman P, Wilson JR, Xue H, Ugander M, Arai AE. Extracellular volume fraction mapping in the myocardium, Part 1: Evaluation of an automated method. J Cardiovasc Magn Reson 2012;14:63.
6. Messroghli DR, Radjenovic A, Kozerke S, Higgins DM, Sivananthan MU, Ridgway JP. Modified Look-Locker inversion recovery (MOLLI) for high-resolution T1 mapping of the heart. Magn Reson Med 2004;52:141–146.
7. Messroghli DR, Greiser A, Fröhlich M, Dietz R, Schulz-Menger J. Optimization and validation of a fully-integrated pulse sequence for modified Look-Locker inversion-recovery (MOLLI) T1 mapping of the heart. J Magn Reson Imaging 2007;26:1081–1086.
8. Silver MS. Highly selective Pi/2 and Pi pulse generation. J Magn Res 1984;59:347–351.
9. Garwood M, Ke Y. Symmetric pulses to induce arbitrary flip angles with compensation for RF inhomogeneity and resonance offsets. J Magn Reson 1991;94:511–525.
10. Tannús A, Garwood M. Improved performance of frequency-swept pulses using offset-independent adiabaticity. J Magn Reson A 1996;120:133–137.
11. Tannús A, Garwood M. Adiabatic pulses. NMR Biomed 1997;10:423–434.
12. Tesiram YA. Implementation equations for HS*n* RF pulses. J Magn Reson 2010;204:333–339.
13. Tesiram YA, Bendall MR. Universal equations for linear adiabatic pulses and characterization of partial adiabaticity. J Magn Reson 2002;156:26–40.
14. Hwang TL, van Zijl PC, Garwood M. Fast broadband inversion by adiabatic pulses. J Magn Reson 1998;133:200–203.
15. Simonetti OP, Kim RJ, Fieno DS, Hillenbrand HB, Wu E, Bundy JM, Finn JP, Judd RM. Cardiac imaging technique for the visualization of myocardial infarction. Radiology 2001;218:215–223.
16. Kim RJ, Shah DJ, Judd RM. How we perform delayed enhancement imaging. J Cardiovasc Magn Reson 2003;5:505–514.
17. Deichmann R, Haase A. Quantification of Tl values by SNAPSHOT-FLASH NMR imaging. J Magn Reson 1992;612:608–612.
18. Kaptein R, Dijkstra K, Tarr C. A single-scan Fourier transform method for measuring spin-lattice relaxation times. J Magn Reson 1976;24:295–300.
19. Gai ND, Stehning C, Nacif M, Bluemke DA. Modified Look-Locker T(1) evaluation using Bloch simulations: human and phantom validation. Magn Reson Med 2013;69:329–336.
20. Chow K, Flewitt J, Pagano JJ, Green JD, Friedrich MG, Thompson RB. T2-dependent errors in MOLLI T1 values: simulations, phantoms, and in-vivo studies. J Cardiovasc Magn Reson 2012;14 (Suppl 1):P281.
21. Cunningham CH, Pauly JM, Nayak KS. Saturated double-angle method for rapid B1+ mapping. Magn Reson Med 2006;55:1326–1333.
22. Sung K, Nayak KS. Measurement and characterization of RF nonuniformity over the heart at 3T using body coil transmission. J Magn Reson Imaging 2008;27:643–648.
23. Hernando D, Kellman P, Haldar JP, Liang Z-P. Robust water/fat separation in the presence of large field inhomogeneities using a graph cut algorithm. Magn Reson Med 2010;63:79–90.
24. Stollberger R, Wach P. Imaging of the active B1 field in vivo. Magn Reson Med 1996;35:246–251.
25. Garwood M, DelaBarre L. The return of the frequency sweep: designing adiabatic pulses for contemporary NMR. J Magn Reson 2001;153:155–177.
26. Rodgers CT, Piechnik SK, Delabarre LJ, Van de Moortele PF, Snyder CJ, Neubauer S, Robson MD, Vaughan JT. Inversion recovery at 7 T in the human myocardium: measurement of T(1), inversion efficiency and B(1) (+). Magn Reson Med 2012. doi: 10.1002/mrm.24548.